Mechanical properties, water absorption and adhesive properties of diepoxy aliphatic diluent-modified DGEBA/Cycloaliphatic amine networks on 316 L stainless steel

Andrés Felipe Espinosa Pineda [a], Filiberto González Garcia [a,*], Alexandre Zirpoli Simões [b], Elson Longo da Silva [c]

[a] Institute of Physics and Chemistry, Federal University of Itajubá, Ave BPS 1303, Itajubá, 37500-903 MG, Brazil
[b] Faculty of Engineering Guaratinguetá, Universidade Estadual Paulista, Ave. Dr. Ariberto Pereira da Cunha 333, Guaratinguetá, 12516-410 São Paulo, SP, Brazil
[c] Paulista State University, Institute of Chemistry, Rua Francisco Degni, 55, Quitandinha, 14801-907 Araraquara, SP, Brazil

ABSTRACT

In this study, the mechanical behaviors, adhesive properties and water absorption of networks based on diglycidyl ether of bisphenol A (DGEBA) modified with diepoxy aliphatic diluent (1,4-butanediol diglycidyl ether, DGEBD) cured with cycloaliphatic amine were studied. The mechanical behaviors and adhesive properties were evaluated by compression testing and single lap-shear using 316 L stainless steel as the adherend, respectively. Water absorption was evaluated by water immersion at 37 ± 0.2 °C. The fracture mechanisms of the networks were determined by optical microscopy. Decreases in the glass transition temperature (T_g) and the yield stress (σ) were noted with increased additive concentrations. The best mechanical performance, accompanied by slight increased adhesive strength, was obtained with 30 phr of additive. The DGEBA/4MPip network modified with 30 phr of diluent shows the best compressive behavior, adhesive strength, and lower water absorption. This behavior may relate to the lower crosslinking density resulting from the reaction mechanism, of stepwise and addition polymerization. Greater participation of cohesive fracture mechanisms was observed in the epoxy networks modified with 30 phr of additive.

© 2016 Elsevier Ltd. All rights reserved.

1. Introduction

Epoxy formulations are extensively used in adhesives, surface coatings, and composite materials because they have excellent adhesion and mechanical properties [1]. Strong adhesion to a variety of surfaces results from the polarity of the formulations and the polar groups present in the polymer structure. This provides good adhesion to different substrates and compatibility with other materials. In formulations for adhesives and surface coating purposes, the incorporation of diluents is typical [2]. The diluents used are classified as non-reactive or reactive; the former acts as a plasticizer, while the latter modifies the crosslinking density and decreases the viscosity of the formulation [2,3]. Low viscosity is necessary to achieve an even surface coating with good adhesive properties; it also eases processing. Lower-viscosity formulations promote the decreased thickness of films, with improves the adhesion of the films to the substrates. The wettability of the epoxy formulation is increased because of the decreased surface tension of the adhesive compared to the free energy of the substrate.

To obtain high adhesive strength using adhesive joints, different physicochemical parameters such as viscosity, roughness, relative humidity, and adhesive thickness must by controlled [4–7]. Controlling the configurations and joint design is equally necessary; the durability of the joint and a high water uptake capacity are also important [8–10]. The structure-joining can be optimized by a particular service [11–13]. However, determining the relationship between the concentration of reactive diluents on the contact angle, viscosity, and adhesive strength of an adhesive joint eases the design of the product.

Numerous studies have been published on the mechanical properties [14–18], adhesiveness [7,18,19], water absorption [20–22], and adhesive applications of epoxy polymers, particularly for metals and stainless steel as adherends [23–25]. However, to our knowledge, the relationship between diepoxy aliphatic diluent-modified diglycidyl ether of bisphenol A/cycloaliphatic amine network structures, adhesion to 316 L stainless steel, and water absorption behavior have not been characterized.

In this study, three cycloaliphatic amines were selected as curing agent; this curing agent variety has shown good cytotoxicity and antithrombotic properties necessary for cardiovascular applications (e.g., coronary stents) [26]. In the work reported here different properties were tested. The mechanical behaviors were evaluated by compression tests. The adhesive properties were evaluated by single lap-shear tests using 316 L stainless steel as adherend. The water absorption capacity was evaluated by water immersion at 37 ± 0.2 °C. The failure mechanisms in the adhesive joints were analyzed by optical microscopy with imaging software.

In order to maintain a low functionality in the cycloaliphatic amine, the compound 4-methylpiperidine (4MPip) was selected. The other cycloaliphatic amines were based on isophorone diamine (IPD) and 4,4'-diamino-3,3'-dimethyldicyclohexylmethane (3DCM), both having cyclic structures.

Thus, three diepoxy aliphatic diluent-modified epoxy matrices based on diglycidylether of bisphenol A (DGEBA) were studied. Two high-T_g epoxy networks, cured with IPD and 3DCM, and one low-T_g epoxy network, cured with 4MPip were evaluated. The influence of additive concentration on the viscosity, contact angle, mechanical properties, and adhesive strength of DGEBA/3DCM networks were evaluated. We then focused on the relationships between the modification of three epoxy matrix structures with 30 phr of additive and the mechanical behavior, adhesive properties, and water absorption of the structures. Finally, the failure mechanisms in the adhesive joints formed by all epoxy networks were characterized by imaging methods.
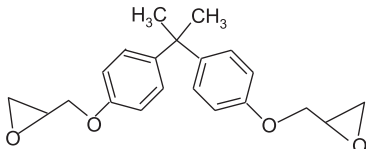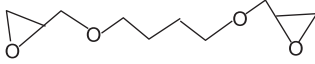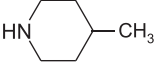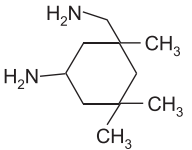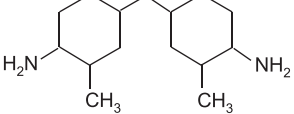
2. Experimental

2.1. Materials

Diglycidyl ether of bisphenol A (DGEBA, DER 331) and diepoxy aliphatic diluent (1,4-butanediol diglycidyl ether, DGEBD, Aldrich), which have epoxy equivalent weights of 185.5 g eq-1 and 123.4 g eq-1, respectively, as determined by acid titration, were used as the epoxy monomer and additive, respectively, in all studied formulations.

The comonomers used as curing agents were the cycloaliphatic tertiary amine, 4-methylpiperidine (4MPip, Aldrich) and two cycloaliphatic primary diamines, isophorone diamine (IPD, Aldrich) and 4,4'-diamino-3,3'-dimethyldicyclohexylmethane (3DCM, Aldrich). IPD and 3DCM have amine-hydrogen equivalent weights of 42.6 g eq^{-1}, and 59.6 g eq^{-1}, respectively, as determined by potentiometric titration in an aqueous medium [27]. The chemical structures, suppliers, purities, molecular weights, and functionalities of the monomers are listed in Table 1. Reagents including 3-aminopropyl-trimethoxysilane (ATPS, 97%, Aldrich, São Paulo, Brazil) and acetone, and analytical-grade 95% ethanol were used as received. The medical-grade 316 L stainless steel was the commercial VI 138 stainless steel (specialty alloy, ASTM –

Table 1
Chemical structure and characteristics of the various monomers.

Monomers	Chemical Structure	Supplied	M g. mol^{-1}	F
Diglycidyl ether of bisphenol A (DGEBA)		Dow Chemical DER 331	~371.00	2
Diglycidyl ether of 1,4-butanediol (DGEBD)		Aldrich (60.0%)	202.25	2
4-Methylpiperidine (4MPip)		Aldrich (96.0%)	98.17	1
Isophorone diamine (IPD)		Aldrich (99.0%)	170.30	4
4,4'-Diamino-3,3'-dimethyldicyclohexylmethane (3DCM)		Aldrich (99.0%)	238.41	4

M: molecular weight; F: functionality.

F138) from Villares Metals, Brazil. The steel was supplied in sheets of 1.0 m length, 12.0 mm width, and 1.6 mm thickness with unpolished surfaces.

2.2. Specimens preparation

Four formulations were prepared with 0, 10, 20, and 30 g additive per 100 g epoxy monomer (parts per hundred of epoxy monomer or phr) in the epoxy monomer mixture. The first series of epoxy monomer mixtures were prepared by adding a stoichiometric amount of curing agent 3DCM (ratio of epoxy/amine hydrogen $e/a=1$) and mixing at room temperature (25 °C) until a homogeneous liquid was obtained. For each formulation, appropriate amounts of the compounds were degassed at room temperature under magnetic stirring for 5 min. The mixture was then poured into a silicone mold, cured in a forced-air oven at 60 °C for 4 h, submitted to a post-cure state at 180 °C for 2 h, and cooled slowly to room temperature. Specimens for mechanical and water absorption testing were machined as plates or cylinders from the molded materials, to reach the final required dimensions and improve the surface finish. The cure schedule utilized was estimated from previous DSC studies. The glass transition temperature (T_g) of the unmodified DGEBA/3DCM network was 174.5 °C, as measured at the midpoint of the transition, in accordance with others studies [28,29].

A similar procedure was used for preparing the second and third series specimens, using a formulation with 30 phr additive in the epoxy monomer mixture. The second series of epoxy monomer mixture was prepared by adding a stoichiometric amount of curing agent IPD (ratio of epoxy/amine hydrogen $e/a=1$) and cured for 4 h at 60 °C and 2 h at 160 °C. The third series was prepared by adding 5 phr 4MPip and cured for 30 min at 60 °C and 16 h at 120 °C.

2.3. Determination of physicochemical parameter

Metallic surfaces were prepared in order to reproduce surface coatings on 316 L stainless steel, which is typically used for medical applications (e.g., on stent coronaries). Unpolished 10.0 mm × 10.0 mm × 1.2 mm plates were ultrasonically cleaned in acetone for 10 min and dried by dabbing with absorbent paper. One surface of each plate was mechanically polished to a mirror-like finish using a succession of 230, 300, 400, 500, 600, and 1200 silicon carbide disks, followed by 0.30 μm and 0.05 μm alumina particles (suspended in solution). To remove residual polishing media, the samples were cleaned with distilled water between each polishing step. They were then dried by dabbing with absorbent paper. The cleaned and polished metal surface was chemically treated in a sulfochromic bath (97% sulfuric acid, and 3% potassium dichromate) at 60 °C for 10 min, rinsed with distilled water, and blown dry with nitrogen gas. After the chemical treatment, the samples were silanized by a silane solution (ATPS, 0.12% v/v) in a mixture of ethanol and distilled water at 25/75% (v/v), according to the methodology reported elsewhere [30]. The treated plates were stored in a glass dryer with silica gel until testing began.

On the polished surface of the treated plate, one drop of the freshly prepared epoxy formulation was deposited using a micropipette; the contact angle was measured at 25 °C. Measurements were obtained less than 1 min after the homogenization of each formulation under equilibrium conditions. The measuring equipment used was a Kruss, model FMMK2 Easydrop equipped with a camera and software for the contact angle measurement.

The viscosity of the epoxy formulations was measured using a rheometer, (Physica Anton Paar, model MCM 301) at 25 °C with conical plates of 24.74 mm diameter and angle 1.012°. The measurements were taken less than 1 min after homogenization of each formulation at a shear rate of 50 s^{-1} for 2 min.

2.4. Mechanical tests

The specimens were tested to fracture under compression conditions. Mechanical testing was performed by a universal testing machine, EMIC model DL 2000, with a 5.0 kN load cell. Measurements were performed for each sample at 50 ± 5% relative humidity at 23 ± 2 °C. The compression stress (σ), compression strain (ε) and maximum strain (ε_{max}) values were determined following the ASTM D695 standard at 1.0 mm min^{-1} using cylindrical specimens 20.0 ± 0.2 mm long with, 10.0 ± 0.2 mm diameters. The reported values were averaged from measurements of at least six specimens.

2.5. Preparation of lap shear specimens

The 316 L stainless steel used was a commercial stainless steel VI 138 (specialty alloy, ASTM – F138) from Villares Metals, Brazil.

The composition of the 316 L stainless steel alloy is given in Table 2. In order to increase the adhesive properties, the metallic adherend surfaces were treated by ultrasonically cleaning in acetone at room temperature for 5 min, dipped in acetone at 40 °C for 5 min, and dried by dabbing with absorbent paper and a dry nitrogen flow. The metal plate surfaces were then chemically treated in a sulfochromic bath and silanized as described in Section 2.3. The specimens were stored in a glass dryer with silica gel until testing.

The adhesive behavior was monitored using single-lap shear joints. The adhesion test was performed according to ASTM D 1002-01. The geometry of the adhesive joint is shown in Fig. 1. For adhesive applications, a metallic mold was designed for the specific adhesive joint. The design of the mold allows the exact control of the layer thickness of the adhesive. After surface treatment, the metallic pieces were assembled in the adhesive single-lap shear joint. The epoxy adhesives were prepared as mentioned in Section 2.2.

The epoxy formulation was applied uniformly on both surfaces of the steel adherends in the molds. The applied contact pressure was kept constant, which provided specimens with a uniform adhesive thickness of 0.2 ± 0.04 mm. The specimens in the molds were cured as described in Section 2.2. To reduce deviation in the adhesive layer with respect to the tensile axis, chocks were placed at the extremes of the specimens. Before testing, the specimens were stored at 22 ± 2 °C and relative humidity of 50 ± 5% for 48 h.

2.6. Testing of the adhesive specimens

The adhesive strength of the single-lap shear joints was measured at room temperature using a universal testing machine under a 5 kN load cell. The crosshead speed was 3.0 mm min^{-1}. The lap shear strength was expressed in MPa. The adhesion tests were performed at 23 ± 2 °C and of 50 ± 5% relative humidity. The reported values were averaged from tests of at least five specimens.

2.7. Evaluation of the failure surface

The failure mechanisms of the different adhesive joints were determined by optical microscopy (Topcon) with imaging analysis software. The fracture surfaces were observed and recorded by

Table 2
Chemical composition in wt% of the 316 L stainless steel.

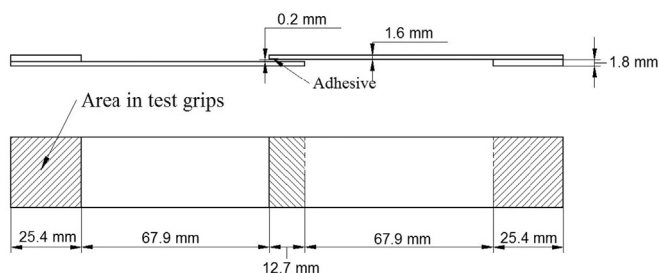| C	Mn	Si	Cr	Ni	Mo	P	S	Cu	N
0.013	1.77	0.028	17.33	14.51	2.78	0.023	0.0010	0.08	0.083

Fig. 1. Dimensions of the adhesives joints of single lap-shear using 316 L stainless steel adherend (measured in mm).

optical microscopy. The images were transmitted by a video camera to a personal computer. The dark and clear regions were attributed to cohesive and adhesive failure, respectively. The percentage of cohesive failure was calculated as the quotient of the dark areas and the total area of the metal substrate multiplied by 100.

2.8. Water absorption

Test specimens of 10.0 ± 0.2 mm $\times$ 15.0 ± 0.2 mm $\times$ 3.2 ± 0.2 mm were used for water absorption tests, following the recommendations of the ASTM D570 standard for testing specimens of sheet materials. The samples were removed at regular intervals from a bath of distilled water at 37.0 ± 0.2 °C, carefully wiped with a filter paper, and weighed on an analytical balance with a precision of ± 0.01 mg. Three specimens of each epoxy polymer were tested.

2.9. Differential scanning calorimetric

The glass transition temperature (T_g) of the specimens in the form of samples weighing 10 ± 2 mg was determined by a differential scanning calorimetric Shimadzu, model DSC-60 at 10 °C min^{-1} under dry nitrogen flowing at 50 mL min^{-1} from room temperature to 250 °C. T_g was taken as half the height (middle point) of the change in heat capacity.

3. Results and discussion

3.1. Mechanical properties

Table 3 lists the values of T_g and mechanical properties of the DGEBA/3DCM networks with different concentrations of diepoxy aliphatic diluent. The values reported are averages of the results from multiple specimens. Increasing the additive concentration decreases both T_g and yield stress (σ). T_g decreases from 174.9 °C to 142.3 °C and σ decreases from 91.4 MPa to 80.4 MPa as the additive amount increases from 0 phr to 30 phr. However, maximum strain (ε_{max}) remains constant for any amount of additive, in agreement with literature data [29].

In this case, the diepoxy aliphatic diluent in the epoxy networks provokes the formation of chains between two crosslinks with greater spacing. This effect increases with the concentration of the diepoxy additive, increasing the concentration of chains and decreasing the crosslinking density. It follows that the additive changes the flexibility; consequently, σ and Tg both decrease gradually. However, low-Tg epoxy networks are known to result from lower crosslinking density [31]. This also explains the increased ($\varepsilon = 8.4\%$) and decreased ($\sigma = 80.4$ MPa) by the increase of the additive concentration to 30 phr. With these results, we selected an additive concentration of 30 phr as the most promising

Table 3
Glass transition temperature (T_g) and compressive mechanical properties of DGEBA/3DCM networks with different concentrations of additive.

Epoxy networks	T_g (°C)	σ (MPa)	ε (%)	ε_{max} (%)
DGEBA/3DCM[a]	174.9	91.4 ± 0.7	6.4 ± 0.3	39.1 ± 0.3
DGEBA/3DCM[b]	154.2	87.6 ± 0.4	7.2 ± 0.2	40.9 ± 0.2
DGEBA/3DCM[c]	149.7	81.6 ± 0.5	7.9 ± 0.3	41.0 ± 0.3
DGEBA/3DCM[d]	142.3	80.4 ± 0.4	8.4 ± 0.1	41.4 ± 0.1

a, b, c, and d, have 0, 10, 20, and 30 phr of diepoxy aliphatic diluent, respectively. $\sigma, \varepsilon,$ and $\varepsilon_{max} =$ stress, strain, and maximum strain.

Table 4
Glass transition temperature (T_g) and compressive mechanical properties of DGEBA/3DCM, DGEBA/IPD, and DGEBA/4MPip networks with 30 phr of additive.

Epoxy networks	T_g (°C)	σ (MPa)	ε (%)	ε_{max} (%)
DGEBA/3DCM	142.3	91.4 ± 0.7	6.4 ± 0.3	39.1 ± 0.3
DGEBA/IPD	109.5	87.6 ± 0.6	6.8 ± 0.5	54.1 ± 1.0
DGEBA/4MPip	63.5	80.2 ± 0.4	8.4 ± 0.2	60.4 ± 0.8

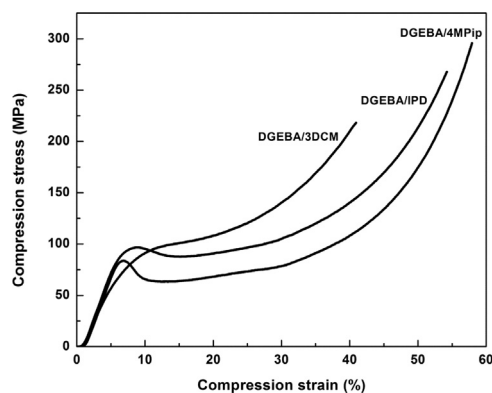$\sigma, \varepsilon,$ and $\varepsilon_{max} =$ stress, strain, and maximum strain.

Fig. 2. The compression stress–strain curves obtained by compression testing of the epoxy networks.

amount for the epoxy networks for obtaining flexible materials with greater adhesive strengths.

Table 4 lists the T_g values and mechanical properties of the DGEBA/3DCM, DGEBA/IPD, and DGEBA/4MPip networks with 30 phr additive. The DGEBA/3DCM and DGEBA/IPD networks show the highest T_g values and similar σ. The DGEBA/4MPip network shows the lowest σ and T_g, but the compressive behavior of the material yields better values when considering the high $\varepsilon =$ of 8.0% and the lower $\sigma =$ of 80.2 MPa. This indicates greater flexibility in the DGEBA/4MPip network. In addition, the DGEBA/IPD network exhibits more flexibility than the DGEBA/3DCM network. This is displayed in Fig. 2, which confirms the greater flexibility of the DGEBA/4MPip network.

The mechanical performances in compressive testing relate to the different structures of the epoxy networks because of the changed comonomer chemical structures and different polymerization mechanisms. The DGEBA/IPD and DGEBA/3DCM networks are generated by the stepwise reaction of amine-hydrogens with epoxy groups, which creates relatively high-T_g epoxy networks with a stoichiometric ratio of the monomers.

The DGEBA/4MPip network operates differently. Two different curing processes occur in the network for epoxy crosslinking, by the stepwise reaction of amine-hydrogens with epoxy groups and by the addition anionic polymerization of the epoxy groups. Despite the high crosslinking density of the network, the high flexibility of the polyether chains creates a low-T_g epoxy network. In these circumstances, the flexible epoxy network chains exhibit a

Table 5
Glass transition temperature (T_g) and adhesives properties of DGEBA/3DCM networks with different additive concentrations and DGEBA/IPD and DGEBA/4MPip networks with 30 phr of additive, obtained from single lap-shear tests.

Epoxy networks	T_g (°C)	Adhesive strength in lap shear joints (MPa)
DGEBA/3DCM (0 phr)	174.9	13.8 ± 0.7
DGEBA/3DCM (10 phr)	154.2	13.9 ± 0.7
DGEBA/3DCM (20 phr)	149.7	14.2 ± 0.6
DGEBA/3DCM (30 phr)	142.3	14.6 ± 0.5
DGEBA/IPD (30 phr)	109.5	15.5 ± 0.4
DGEBA/4MPip (30 phr)	63.5	17.2 ± 0.4

Table 6
Physicochemical properties of viscosity and contact angle of DGEBA/3DCM formulations with different additive concentrations and DGEBA/IPD and DGEBA/4MPip formulations with 30 phr of additive.
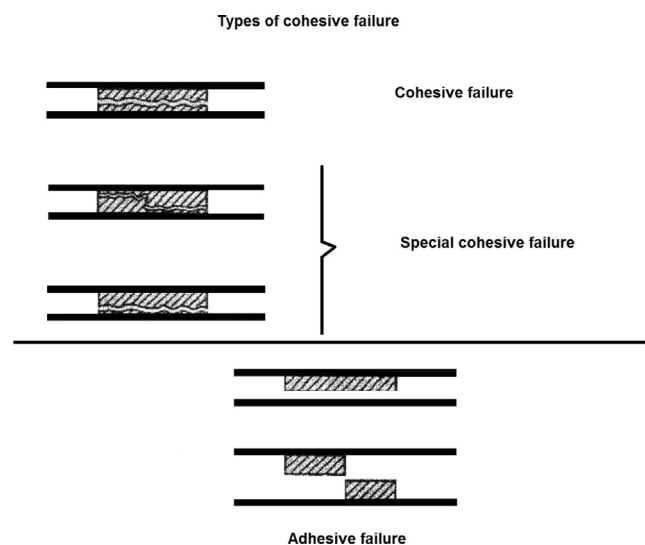
Epoxy formulations	Viscosity (Pa s)	Contact angle (°)
DGEBA/3DCM (0 phr)	3.68	68 ± 4
DGEBA/3DCM (10 phr)	2.52	54 ± 3
DGEBA/3DCM (20 phr)	1.24	50 ± 2
DGEBA/3DCM (30 phr)	0.51	49 ± 2
DGEBA/IPD (30 phr)	0.44	37 ± 3
DGEBA/4MPip (30 phr)	0.54	32 ± 1

lower crosslinking density and T_g. From these results, we can infer the relationship between the mechanical properties and the chemical structures of the comonomers, which changes the structure of the network.

3.2. Adhesive properties

Table 5 lists the adhesive properties of different epoxy formulations, as obtained from the single lap-shear joints tests described in Section 2.6. The T_g of the epoxy networks does not influence the adhesive behavior of the joints. Table 5 also reveals that the T_g values of DGEBA/3DCM networks with different amounts of diepoxy aliphatic diluent are changed with the amount of additive used. Increased additive concentration decreases T_g and does not significantly increase the adhesive strength. T_g decreases from 174.9 °C to 142.3 °C while the adhesive strength increases slightly from 13.8 MPa to 14.6 MPa as the additive amount increases from 0 phr to 30 phr. Table 6 demonstrates that the contact angle and viscosity decreases with increased amounts of additive. With the low viscosity and contact angle we note some improvement of the adhesive strength with the 316 L stainless steel substrate. These physicochemical parameters influence the adhesive strength of the adhesive joints [2,6,32]. Lower viscosities and contact angles are important in achieving surface coatings with high adhesive strength. For example, the diglycidyl ether of glycerol as an epoxy monomer has a low viscosity at room temperature. This monomer was recently investigated for coating applications [33,34].

Meanwhile, the DGEBA/4MPip network exhibits the best adhesive strength compared to the DGEBA/3DCM and DGEBA/IPD networks. The DGEBA/4MPip network shows a lower T_g value (Table 5) and a relatively low viscosity and contact angle (Table 6) compared to other epoxy networks and formulations studied in this work. This relates to the physicochemical parameters of the formulation and the lower crosslinking density improves the adhesion, thus increasing the lap-shear strength [19]. The DGEBA/IPD and DGEBA/3DCM networks show the largest T_g values. However, the DGEBA/IPD network structure exhibits more flexibility than that of the latter, leading to relatively high-T_g equivalent values for viscosity and contact angle, and better adhesive

Fig. 3. Schematic representation depicting types of failure in adhesive joints.

Table 7
Percentage of cohesive failure in the fractured joints with different epoxy networks. DGEBA/3DCM networks used different additive concentrations; DGEBA/IPD and DGEBA/4MPip networks used 30 phr of additive.

Epoxy networks	Cohesive failure (%)
DGEBA/3DCM (0 phr)	78
DGEBA/3DCM (10 phr)	79
DGEBA/3DCM (20 phr)	80
DGEBA/3DCM (30 phr)	82
DGEBA/IPD (30 phr)	78
DGEBA/4MPip (30 phr)	90

properties. This indicates greater flexibility in this network than in the DGEBA/3DCM network.

The adhesive performances relate to the different structures of the epoxy networks, as mentioned in Section 3.1. With the results of this work the mechanical properties and adhesives properties can be related to the changed chemical structures of the comonomers used as curing agents, which provoke structural changes in the networks.

3.3. Characterization of the adherend surface

Fig. 3 illustrates different failures types in the adhesive joints. Failure can occur inside the adhesive layer (cohesive failure with adhesive residues on both surfaces) or at the interface between the adhesive layer and the adherend surface (adhesive failure). The images of the joints after fracture reveal dark and clear regions, corresponding to adhesive and metallic surface, respectively. The prevalence of each surface type is shown numerically in Table 7. As can be seen, the cohesive fracture mechanisms have limited participation in the DGEBA/3DCM networks with different amounts of diepoxy aliphatic diluent for the networks modified with 30 phr of diluent, the participation of cohesive fracture mechanisms is greater. These behaviors may be related to the slight increases of the lap shear strength by the increased additive concentration, as well as the different structures of the epoxy networks because of the lower crosslinking density. As would be expected, cohesive failure dominates in the epoxy networks [9,19,35].
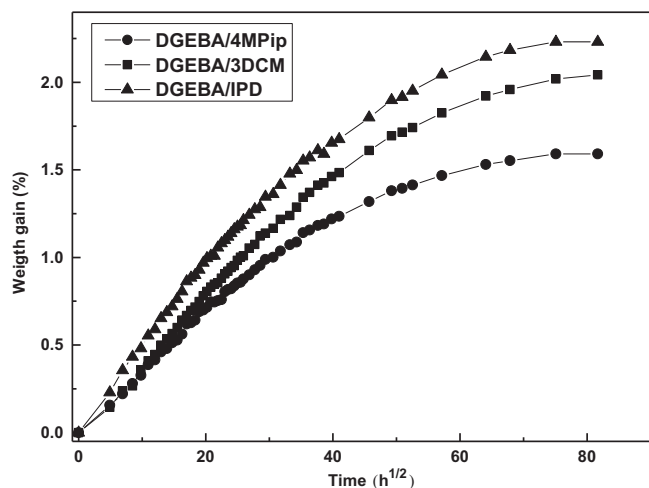
Fig. 4. Weight gain vs. time, showing the water sorption behavior of the different epoxy networks.

3.4. Water absorption

Solvent transport in organic polymer matrices is usually depicted as occurring by a two-step mechanism. In the first step, the solvent dissolves in the superficial polymer layer. This process, which can be considered to occur virtually instantaneously with water as investigated here, creates a concentration gradient. In the second step, the solvent diffuses in the direction of the concentration gradient. This process is described by the differential mass balance expressed in Fick's second law [31,36], which may be written for a one-dimensional case as:

$$\frac{\Delta C_t}{\partial t} = D\frac{\partial^2 C_t}{\partial x^2} \tag{1}$$

where: D is the diffusion coefficient and x the coordinate along the sample's thickness L. For a membrane-shape sample [37], the resolution of this differential equation is expressed as:

$$\frac{C_t}{C_\infty} = 1 - \sum_{n=0}^{\infty}\frac{8}{(2n+1)^2\pi^2}\exp\left[\left(\frac{-D\left(n+\frac{1}{2}\right)^2\pi^2 t}{L^2}\right)\right] \tag{2}$$

For short times frames, typically when the concentration $C \leq 0.5\,C_\infty$, this function is well approximated by:

$$\frac{C_t}{C_\infty} = 1 - \frac{8}{\pi^2}e^{\left(\frac{-D\pi^2 t}{4L^2}\right)} \tag{3}$$

where: C_t is the mass of water absorbed at time t, C_∞ is the amount of water absorbed at saturation, L is the thickness of the free-standing specimen, and D is the diffusion coefficient. It is usual to plot $\ln(1-C_t/C_\infty)$ versus $\ln t$. The linearity of the curve at small $\ln t$ is considered a validity criterion for the application of Fick's second law. The slope of the linear portion allows the determination of the diffusion coefficient. To obtain C_∞ and diffusion time (t_D), weight gain is plotted over time. In this plot, t_D defined as the duration of the transient, can be arbitrarily taken at the intersection of the tangent at the origin and the asymptote; C_∞ is considered the maximum value of the weight gain of the sample. This point corresponds to the value at which the absorption stabilizes.

Fig. 4 shows the experimental data for the weight gain over time. All epoxy polymers show linear relationships between the weight gain and the immersion time initially. This behavior is well described by Eq. (3), showing that the initial stage of water absorption behavior is governed by Fick's second law. Therefore, the water concentration gradient drives water absorption in these epoxy polymers. As seen in Fig. 4, the immersion time used caused saturation in all samples.

Table 8
Diffusion coefficient (D, mm^2/s), saturation value (C_∞, %) and diffusion time (t_D, days) obtained from Fig. 4 of DGEBA/3DCM, DGEBA/IPD, and DGEBA/4MPip networks with 30 phr of additive.

	DGEBA/3DCM	DGEBA/IPD	DGEBA/4MPip
C_∞ (%)	1.497	1.522	1.227
D (mm^2/s) $\times 10^{-6}$	1.176	1.194	0.958
t_D (days)	57.56	54.12	61.04

The obtained values for C_∞, D and t_D are listed in Table 8. Notably, the obtained D is consistent with the values cited for other epoxy polymers [31,38–40]. C_∞, D and t_D change for each epoxy network depending on the comonomer employed. D and C_∞ for DGEBA/4MPip network are always lower than those of the others epoxy networks. However, t_D is the largest for the same network. The DGEBA/3DCM and DGEBA/IPD networks show equivalent D, C_∞ and t_D values.

Some authors have reported that the molecular structures of the comonomers and the degree of crosslinking affect the water absorption [24,41], but have not clearly established the structure-diffusivity relationships. Reports on diffusion kinetics suggest that, in aliphatic diepoxide cured by aromatic diamine, the diffusion rate of water is controlled by the strength of the polymer-water hydrogen bond [42]. In this way, the DGEBA/4MPip network has a little concentration of hydrogen bond [9] because of the two different curing processes, as mentioned previously. This structural characteristic impedes the diffusion rate of water. For the DGEBA/3DCM and DGEBA/IPD networks, the hydrogen bond concentrations are similar, but the first network has a more rigid structure than the latter network, decreasing D, C_∞ and t_D values. This complicates the diffusion rate of water in the DGEBA/3DCM network.

4. Conclusions

The mechanical and adhesive properties of the tested epoxy networks relate to the chemical structures of the comonomers used as curing agents, which change the structures of the networks. Increasing the amount of additive in the DGEBA/3DCM formulation decreases the glass transition temperature, the yield stress, the contact angle value, and the viscosity, while it increases the lap-shear strength and the participation of cohesive fracture mechanisms. The best performance was obtained for the DGEBA/4MPip network modified with 30 phr of the diluent; it showed the greatest participation of cohesive fracture mechanisms, the best compressive behavior, and the highest adhesive strength, and the lowest water absorption.

References

[1] New materials and innovation In: J.P. Pascault R.J.J. Williams(Eds.), Epoxy Polymers 2010 Wiley-VCH Verlang GmbH & Co. KGaA Weinheim.
[2] F. Lewis, Armand, Epoxy Resins. Chemistry and Technology, in: Epoxy Resins Adhesives. Clayton AM. 2nd ed. Marcel Dekker: New York, 1988.
[3] H. Lee, K. Neville. Handbook of Epoxy Resins, in: Flexibilizers and plasticizers for epoxy resins. McGraw-Hill, New York, 1967.
[4] Xu W, Wei Y. Influence of adhesive thickness on local interface fracture and overall strength of metallic adhesive bonding structures. Int J Adhes Adhes 2013;40:158.

[5] Oudad W, Madani K, Bouiadjra BB, Belhouari M, Cohendoz S, Touzain S, Feaugas X. Effect of humidity absorption by the adhesive on the performances of bonded composite repairs in aircraft structures. Compos: Part B 2012;43:3491.

[6] Montois P, Nassiet V, Petit JA, Adrian D. Viscosity effect on epoxy-diamine/metal interphases - Part II: mechanical resistance and durability. Int J Adhes Adhes 2007;27:145.

[7] Lapique F, Redford K. Curing effects on viscosity and mechanical properties of a commercial epoxy resin adhesive. Int J Adhes Adhes 2002;22:337.

[8] Cognard JY, Sohier L, Créac'hcadec R, Lavelle F, Lidon N. Influence of the geometry of coaxial adhesive joints on the transmitted load under tensile and compression loads. Int J Adhes Adhes 2012;37:37.

[9] González Garcia F, Leyva ME, Queiroz AAA, Simões AZ. Durability of adhesives based on different epoxy/aliphatic amine network. Int J Adhes Adhes 2011;31:177.

[10] Zanni-Deffarges MP, Shanahan MER. Diffusion of water into an epoxy adhesive: comparison between bulk behaviour and adhesive joints. Int J Adhes Adhes 1995;15(3):137.

[11] Taib AA, Boukhili R, Achiou S, Gordon S, Boukehili H. Bonded joints with composite adherends. Part I. Effect of specimen configuration, adhesive thickness, spew fillet and adherend stiffness on fracture. Int J Adhes Adhes 2006;26(4):226.

[12] d' Silva LFM, Adams RD. The strength of adhesively bonded T-joints. Int J Adhes Adhes 2002;22(4):311.

[13] Li W, Blunt L, Stout KJ. Analysis and design of adhesive-bonded tee joints. Int J Adhes Adhes 1997;17(4):303.

[14] Liu Y, Yang G, Xiao HM, Feng PQ, Fu SY. Mechanical properties of cryogenic epoxy adhesives: Effects of mixed curing agent content. Int J Adhes Adhes 2013;41(1):113.

[15] González Garcia F, Soares BG, Pita VJRR, Sánchez R, Rieumont J. Mechanical properties of epoxy networks based on DGEBA and aliphatic amines. J Appl Polym Sci 2007;106(3):2047.

[16] Crawford E, Lesser AJ. Brittle to ductile: Fracture toughness mapping on controlled epoxy networks. Polym Eng Sci 1999;39(2):385.

[17] Cook WD, Mayr AE, Edward GH. Yielding behaviour in model epoxy thermosets - II. Temperature dependence. Polymer 1998;39(16):3725.

[18] Yang G, Fu SY, Yang JP. Preparation and mechanical properties of modified epoxy resins with flexible diamines. Polymer 2007;48(1):302.

[19] Hu X, Huang P. Influence of polyether chain and synergetic effect of mixed resins with different functionality on adhesion properties of epoxy adhesives. Int J Adhes Adhes 2005;25(4):296.

[20] Musto P, Mascia L, Ragosta G, Scacarinzi G, Villano P. The transport of water in a tetrafunctional epoxy resin by near-infrared Fourier transform spectroscopy. Polymer 2000;41(2):565.

[21] Zhou J, Lucas JP. Hygrothermal effects of epoxy resin. Part I: the nature of water in epoxy. Polymer 1999;40(20):5505.

[22] Diamant Y, Marom G, Broutmant LJ. The effect of network structure on moisture absorption of epoxy resins. J Appl Polym Sci 1981;26(9):3015.

[23] Morais AB, Pereira AB, Teixeira JP, Cavaleiro NC. Strength of epoxy adhesive-bonded stainless-steel joints. Int J Adhes Adhes 2007;27(8):679.

[24] Fana D., Bockenheirmer C., Possart W., Adhesion, current research and application, in: W. Possart, (ed.) Wiley-VCH Verlang GmbH & Co. KgaA, Weiheim, Germany, vol. 30, 2005, p. 479.

[25] Pereira AB, Morais AB. Strength of adhesively bonded stainless steel joints. Int J Adhes Adhes 2003;23(4):315.

[26] F. González Garcia, M.E. Leyva, A.A.A. Queiroz, O.Z. Higa, J Appl Polym Sci, 2009, 112(9), p. 1215.

[27] González Garcia F, Silva PM, Soares BG, Rieumont J. Combined analytical techniques for the determination of the amine hydrogen equivalent weight in aliphatic amine epoxide hardeners. Polym Test 2007;26(1):95.

[28] Montserrat S, Roman F, Colomer P. Vitrification and dielectric relaxation during the isothermal curing of an epoxy–amine resin. Polymer 2003;44(1):101.

[29] Urbaczewski-Espuche E, Galy J, Gerad FJ, Pascault JP, Sautereau H. Influence of chain flexibility and crosslink density on mechanical properties of epoxy/amine networks. Polym Eng Sci 1991;31(22):1572.

[30] Chovelon JM, Aarch LEL, Charbonnier M, Romand M. Silanization of stainless steel surface: influence of application parameters. J Adhesion 1995;50(1):43.

[31] Pascault JP, Sautereau H, Verdu J, Williams RJJ. Thermosetting Polymers. New York: Marcel Dekker; 2002.

[32] Packhan DE. Work of adhesion: contact angles and contact mechanics. Int J Adhes Adhes 1996;16(2):121.

[33] Omrani A, Rostami A, Ravari F, Ehsani M. The relationship between composition and electrical properties of brass covered by a nanocomposite coating of glycerol diglycidyl ether: an EIS and DMTA study. Prog Org Coat 2013;76:360.

[34] Omrani A, Rostami AA, Ravari F, Mashak A. Curing behavior and structure of a novel nanocomposite from glycerol diglycidyl ether and 3,3-dimethylglutaric anhydride. Thermochim Acta 2011;517:9.

[35] Barcia FL, Soares BG, Sampaio E. Adhesive properties of epoxy resin modified by end-functionalized liquid polybutadiene. J Appl Polym Sci 2004;93:2370.

[36] Shen CH, Springer GS. Moisture adsorption and desorption of composite. J Comp Mater 1976;10:2.

[37] Apostol TM. Mathematic Analysis. United States of America: Addison-Wesley Publishing Company; 1973.

[38] Berry NG, d'Almeida JRM, Barcia FL, Soares BG. Effect of water adsorption on the thermal-mechanical properties of HTPB modified DGEBA-based epoxy systems. Polym Test 2007;26(1):262.

[39] Moy P, Karasz FE. Epoxy-water interactions. Polym Eng Sci 1980;20(4):315.

[40] Maggana C, Pissis P. Water sorption and diffusion studies in an epoxy resin system. J Polym Sci: Part B-Polym Phys 1999;37(1):1165.

[41] Abdelkader AF, While JR. Water absorption in epoxy resins: The effects of the crosslinking agent and curing temperature. J Appl Polym Sci 2005;98(1):2544.

[42] Tcharkhtchi A, Bronnec PY, Verdu J. Water absorption characteristics of diglycidyl ether of butanediol-3,5-diethyl-2,4-diaminotoluene networks. Polymer 2000;41(15):5777.